Distribution in energy and angle of electrons ejected from xenon by 0.3- to 2.0-MeV protons*

L. H. Toburen
Battelle Pacific Northwest Laboratory, Richland, Washington 99352
(Received 14 February 1974)

Absolute cross sections, differential in electron energy and emission angle, have been measured for ejection of electrons from xenon by 0.3- to 2.0-MeV protons. Electron-energy distributions are presented for ten angles between 20° and 130°. Angular distributions are found to be more nearly isotropic than results for targets of lower atomic number. Cross sections differential in electron energy obtained by integration with respect to emission angle, are found to be in relatively good agreement with calculations based on binary-encounter theory. Auger electrons resulting from initial vacancies in the M and N shells of xenon are discussed. Estimates of total M- and N-shell ionization cross sections for fast protons are presented.

I. INTRODUCTION

Absolute cross sections for electron emission to ion-atom collisions provide information concerning ionization processes which play an important role in atmospheric, plasma, and radiological physics. These cross sections, differential in electron-emission energy and angle, are useful for testing theoretical approximations and for practical applications in the investigation of energy transfer by fast charged particles. Previous measurements of double-differential cross sections for incident protons have been confined primarily to targets of low atomic number (i.e., H_2, He, N_2, Ne, Ar); these results were reviewed recently by Rudd and Macek.[1] Theoretical calculations are difficult for even the simplest systems, and only recently have calculations been performed which appear to provide reliable double-differential electron-emission cross sections.[2,3] For more complicated systems, such as molecules and atoms with several electronic shells, the only calculations presently available are single-differential and/or total cross sections obtained from binary-encounter theory. The reliability of these calculations has not been tested for atoms with several electronic shells.

In the present work electron-emission cross sections differential in electron energy and emission angle are reported for 0.3–2.0-MeV protons on xenon. Protons in this energy range produce vacancies primarily in the M, N, and O shells of xenon (principal quantum numbers 3, 4, and 5, respectively). The ionization of M and N shells is deduced from Auger electrons observed in the ejected-electron spectra. No evidence of K- or L-Auger electrons was observed, indicating that the probability of producing K- and L-shell vacancies in xenon is negligible for proton energies from 0.3 to 2.0 MeV.

II. EXPERIMENTAL METHOD

The apparatus and experimental technique used in these measurements has been described previously.[4,5] Protons with energies from 0.3 to 2.0 MeV were obtained from a Van de Graaff generator. The collimated proton beam passed through a differentially pumped target gas cell and was then collected in a shielded Faraday cup. Electrons ejected in the proton-atom collisions were energy analyzed by a cylindrical-mirror electrostatic analyzer and counted with a continuous-channel electron multiplier. From a knowledge of the gas pressure, proton beam intensity, solid angle, and other experimental parameters, the absolute cross sections for electron emission were calculated. The electrostatic analyzer was positioned so as to study electrons ejected at angles ranging from 20° to 130°. Magnetic fields in the vicinity of the target were reduced to a few mG by three mutually perpendicular sets of Helmholtz coils.

The accuracy of the absolute cross sections is estimated as ±20%, based on uncertainties in the experimental parameters involved in the measurement. The uncertainty in the relative values of the cross sections obtained in this measurement (i.e., an estimate of the internal consistency of the measurements) is estimated as ±10%. A detailed description of the uncertainties encountered in these measurements was presented in an earlier paper.[4]

III. DOUBLE-DIFFERENTIAL CROSS SECTIONS

The double-differential cross sections for 0.3-, 1.0-, and 2.0-MeV proton impact on xenon are shown in Figs. 1–3, respectively. The cross sections have been multiplied by the corresponding electron-emission energy to reduce the number of

decades necessary for plotting. The basic feature of these spectra is a continuous distribution of electrons which peaks for low-energy electron emission and displays a broad secondary maximum for high-energy electron ejection into forward angles. Also evident are Auger electron peaks superimposed on the continuum distributions. These Auger groups correspond to cascades following initial vacancies in the N shell (N-Auger electrons with energies of 30–50 eV) and M shell (M-Auger electrons with energies of 400–500 eV). These Auger lines will be discussed in more detail in Sec. VI. The broad maximum at high energies in the distribution of continuum electrons corresponds to electrons ejected with energies characteristic of direct proton-electron collisions. For a free electron this peak would be a δ-function distribution in electron energy occurring at an ejection energy defined by the collision kinematics. The width of the observed distribution indicates primarily the effects of the momentum distribution of the electrons in the xenon atom. For the low-energy electron cross sections shown in Figs. 1–3, the product of electron energy and emission cross section is nearly independent of electron energy below approximately 10 eV. This feature indicates that the continuum emission cross sections increase monotonically for electron energies as low as 2–4 eV. It should be pointed out that uncertainties in the measured cross sections become larger at the lowest energies measured, so that the exact shape of the spectra at very low energies is not clear. The cross sections for electron energies less than 5 eV are uncertain by as much as a factor of 2, whereas the cross sections for electron energies greater than 10 eV should be accurate to ±20%.

The angular dependence of cross sections for ejection of electrons of several different energies by 0.3-MeV protons is shown in Fig. 4. Also shown in Fig. 4 are results previously published for electron ejection from hydrogen.[6] Both the xenon and hydrogen cross sections exhibit a broad peak in the angular distributions corresponding to the kinematic peak observed in the energy distributions. The xenon cross sections, however, show a much smaller variation with angle than the hydrogen cross sections. For example, for 50-eV electron emission the xenon cross sections vary by only a factor of 3 between the 20° and 130° angles, whereas the hydrogen cross sections differ by more than an order of magnitude. This behavior is even more striking for higher electron energies where the cross sections observed for emission of electrons for large angles from xenon are very large compared to the hydrogen results. It should be noted that this trend, i.e., the emission cross sections becoming more isotropic as the complexity of the target atom increases, has also been observed for nitrogen, oxygen, neon, and argon targets.[4,7] It was suggested in Ref. 7 that the variation in the angular distributions for different target atoms or molecules may be a result of differences in binding energy, differences in the angular momentum of the outer shells, or the presence of inner shells.

The effect of the binding energy on the angular distribution is not obvious. Crooks and Rudd[7] speculate that the "binary-encounter peak," the peak associated with direct proton-electron col-

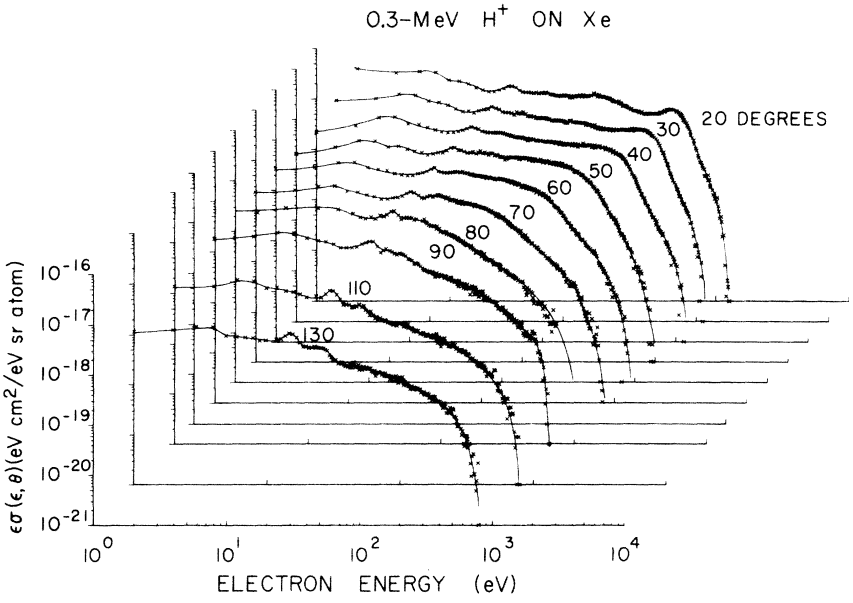

FIG. 1. Cross sections, differential in electron energy and emission angle, for ejection of electrons from xenon by 0.3-MeV protons.

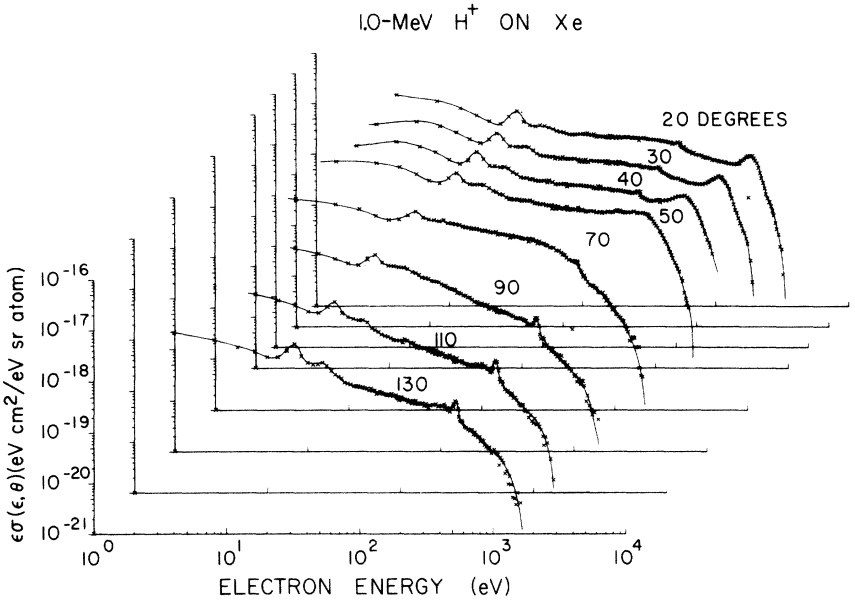

FIG. 2. Cross sections, differential in electron energy and emission angle, for ejection of electrons from xenon by 1.0-MeV protons.

lision, should be most sharply peaked for an atom or molecule with the smallest ionization potential. This conclusion follows from the argument that a stationary free (unbound) electron interacting with the incident proton would lead to a δ-function distribution in angle. The results shown in Fig. 4 do not follow this trend if the ionization potential of xenon is taken as the first ionization potential ($V_{\text{ion}} = 12.127$ V), which is smaller than the ionization potential of hydrogen ($V_{\text{ion}} = 15.4$ V). However, since these energetic incident protons remove electrons from inner shells as well as the outermost, it is more realistic to consider an effective ionization potential for fast protons on xenon. An estimate of the effective ionization potential of xenon for 0.3-MeV protons was made using the expression

$$V_{\text{ion eff}} = \frac{\sum_i (B_i)\sigma_i(\epsilon)}{\sigma_T(\epsilon)} , \tag{1}$$

where B_i is the binding energy of the ith shell, $\sigma_i(\epsilon)$ is the cross section for ejection of an electron of energy ϵ from the ith shell, and $\sigma_T(\epsilon)$ is the total cross section for ejection of an electron of energy ϵ by the incident proton. Values of $\sigma_i(\epsilon)$ and $\sigma_T(\epsilon)$ were estimated using binary-encounter theory, and values of B_i were taken from the table of Sevier.[8] From these estimates the

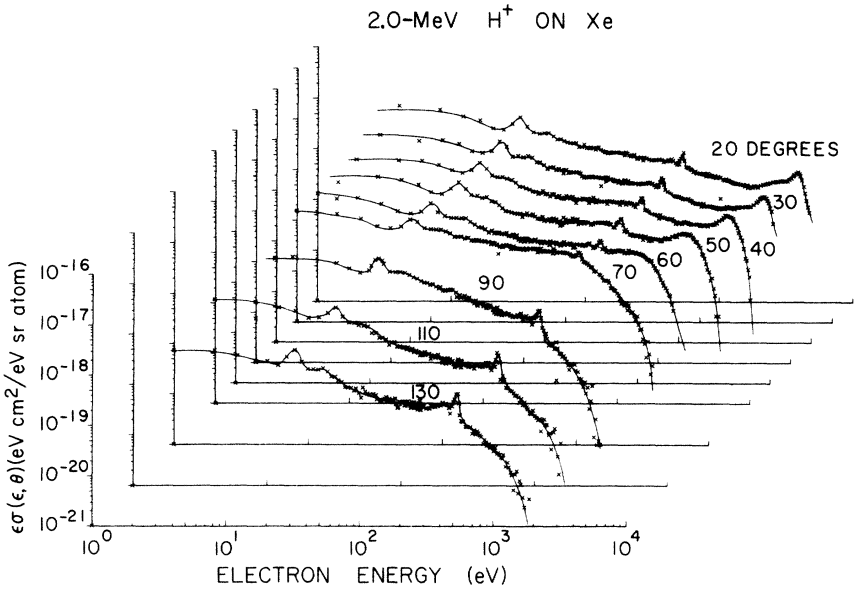

FIG. 3. Cross sections differential in electron energy and emission angle, for ejection of electrons from xenon by 2.0-MeV protons.

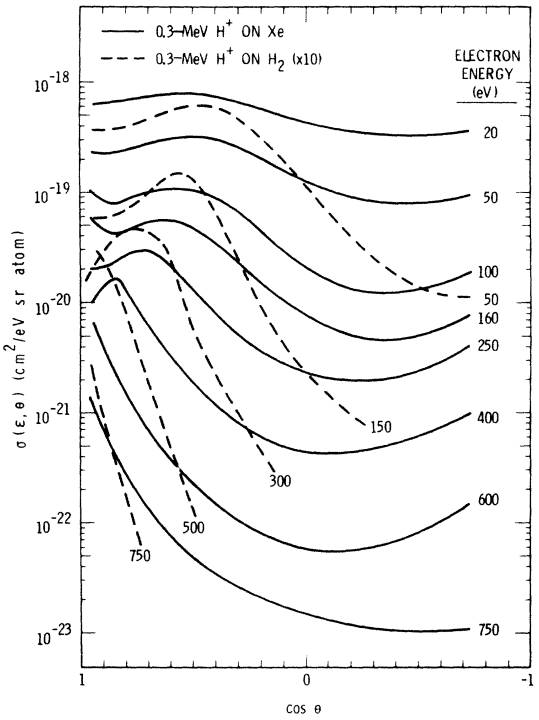

FIG. 4. Angular distributions of electrons of several energies ejected from xenon by 0.3-MeV protons. The dashed lines represent electrons ejected from hydrogen by 0.3-MeV protons. The hydrogen data are from Ref. 6.

effective ionization potential of xenon is approximately 40 V, which is considerably larger than the corresponding value for hydrogen. It then follows that a broader maximum in the binary-encounter peak is to be expected for xenon than for hydrogen.

It is also observed that the binary-encounter peak associated with a particular ejected-electron energy is shifted to slightly smaller angles for xenon than for hydrogen. This result can also be explained by the effectively higher ionization potential of xenon. In order to transfer adequate energy to overcome the higher binding energy, a somewhat smaller impact parameter is required, which results in ejection of electrons into smaller angles.

For low-energy ejected electrons, the angular distribution becomes nearly isotropic, with only small evidence of a binary-encounter peak. These results may be explained in terms of energy being deposited in the atom as a whole by interactions with the proton at large distances, rather than by the more direct proton-electron interactions which lead to the binary-encounter peak. In this case, the angular distributions become smeared by the effects of electron-electron correlation within the atom or by the distortion of the atomic electron distributions by the impulsive interaction with the passing proton.[9,10] In either case, it would follow that a target with a large number of electrons may yield a more nearly isotropic low-energy-electron spectrum. It is unfortunate that our present apparatus does not provide more reliable results for electron energies below about 10 eV, since it would be interesting to determine if lower-energy electrons are even more nearly isotropic.

The emission of low-energy electrons by impact of charged particles has recently been investigated in the dipole approximation by Kim.[11] Since low-energy electrons are ejected in "soft" or glancing collisions at large impact parameters with small momentum transfer, Kim suggests that these soft charged-particle collisions produce ionization in a manner similar to photoionization. One would then expect soft collisions to be described by the dipole contribution to the Born calculation Kim has shown that, for double-differential electron-emission cross sections in the dipole approximation, electrons ejected at any given angle should exhibit a $(\ln T)/T$ dependence and at angles symmetric to 90° the slope of the $(\ln T)/T$ dependence should be the same. For proton impact, T is proportional to the proton energy, i.e., $T=\frac{1}{2}mv^2$, where m is the electron mass and v is the proton velocity. In Fig. 5 are plots of $T\sigma(\epsilon,\theta)$ vs $\ln(T/R)$, for protons on xenon (R is the Rydberg constant). For electrons ejected with kinetic energy of 16 eV, we find excellent agreement with the predictions of Kim's theory; the slopes of the curves are, indeed, the same for electrons ejected at angles symmetric about 90°. For larger ejected-electron energies the slope of the line for electrons ejected into angles smaller than 90° decreases faster than for electrons ejected into the symmetric large angle. A possible explanation of the reduced slope for electrons ejected at forward angles relative to the supplementary angle may be associated with long-range proton-electron interactions which are not described by the Born approximation. An enhancement in small-angle electron-emission cross sections for ejection of electrons having velocities close to that of the incident projectile has previously been observed and discussed in theoretical terms.[12-14] Although this enhancement of emission cross sections is maximal for small ejection angles and for electron velocities equal to the proton velocity, it is conceivable that this long-range interaction also influences the results for lower-energy electrons, such as those considered in Fig. 5. The electron energies which correspond to electrons with velocities similar to the protons are 160, 540, and 1080 eV for 0.3-, 1.0-, and 2.0-MeV protons, respectively. Since the 0.3-MeV proton velocities

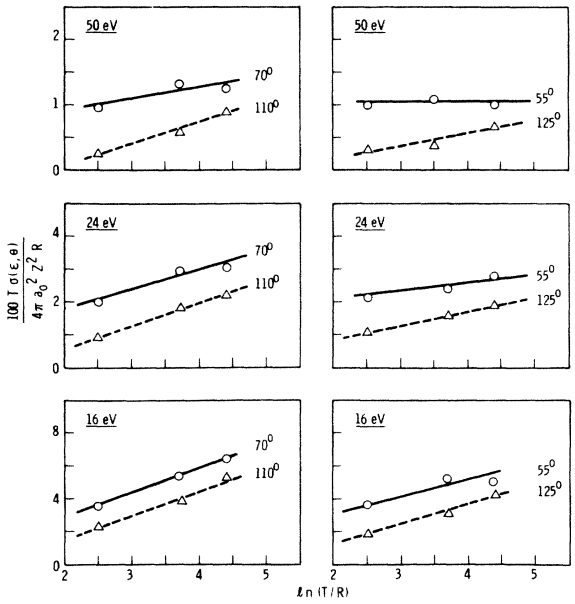

FIG. 5. Comparisons of $T\sigma(\epsilon,\theta)$ vs $\ln(T/R)$ plots for low-energy electrons ejected in fast proton-xenon collisions.

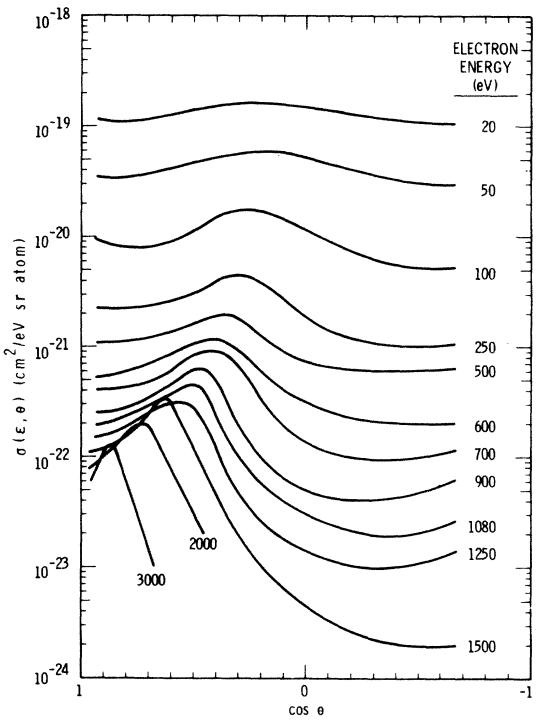

FIG. 6. Angular distributions of electrons of several energies ejected from xenon by 2.0-MeV protons.

are nearest to the corresponding electron velocities considered in Fig. 5, it is expected that the ejection cross sections would be enhanced most for 0.3-MeV proton impact. The long-range interaction between the outgoing proton and ejected electron would therefore tend to reduce the slope of the lines obtained for forward angles over backward angles. This argument would predict larger variations as the electron energy increases and as the emission angle is reduced. Since this trend is observed in Fig. 5, it is probable that the divergence from the predictions of the dipole approximation is due to the long-range proton-electron interactions, which are not included in the Born approximation. This hypothesis is reinforced by the fact that the dipole representation was shown to be adequate in describing the ejection of electrons of the energies considered in Fig. 5, by incident electrons where the long-range interaction is not encountered.[11]

As indicated above, the increase in emission cross sections for small angles, particularly for electron energies corresponding to electrons with velocities similar to the incident-proton velocity, has been observed by Crooks and Rudd[12] and discussed theoretically by Macek[13] and Salin.[14] These authors were concerned primarily with electron emission from hydrogen and helium, where a sharp increase in the electron cross sections was noted for small angles. The results shown in Fig. 4 for 0.3-MeV protons on xenon and in Fig. 6 for 2.0-MeV protons on xenon do not show the dramatic increases observed in the work of Crooks and Rudd[12] for protons on helium. However, evidence for an enhancement of the cross sections appears at somewhat larger angles for xenon than for the simpler systems of hydrogen and helium.

For electrons ejected with intermediate energies there is also an enhancement of cross sections for electron emission into large angles for the higher-Z targets compared to earlier measurements on simpler target systems. For example, the cross sections for emission of 400-eV electrons at 130° shown in Fig. 4 are several orders of magnitude larger for xenon than for hydrogen. Recent calculations using the Born approximation and Hartree-Fock wave functions[2] have shown large contributions for large-angle electron ejection due to interference of various partial waves contributing to the emission cross section. These interference terms do not occur in hydrogenic calculations. Another effect which may influence the angular distributions is the distortion of the electron distribution by the Coulomb potential of the passing proton. One could argue that this distortion would be much greater for xenon than for the simpler hydrogen system. In the case of xenon, the ejection of electrons from inner shells may also be important in determining the shape of the angular distributions. The fact that inner shells are being ionized is evident from the Auger

lines observed in Figs. 1–3. Auger transitions result in the ejection of electrons which are essentially isotropic.

Since the cross sections plotted in Figs. 4 and 6 reflect all electrons ejected from the target, it is possible that Auger electrons contribute sufficiently to dominate at the backward angles. An estimate of the Auger contribution for 400-eV electron emission at 130° (0.3-MeV proton impact) is approximately 3×10^{-22} cm^2/eV sr. This accounts for only about half of the observed cross section. Angular distributions of ejected electrons of several energies are shown in Fig. 6 for 2.0-MeV proton impact. For protons of this energy there is an enhancement of the large-angle electron-emission cross sections for electron energies as large as 1500 eV. These cross sections are not dominated by Auger electrons, since there are no Auger transitions which result in ejection of electrons of 1500 eV. This evidence would tend to diminish the importance of Auger electrons as the cause of the enhancement of large-angle cross sections, although they obviously do contribute in limited regions of the energy spectra.

Electrons ejected directly from inner shells may also influence the angular distribution. The angular distributions of these electrons, however, is not known. Until electron spectra can be measured which separate electrons from the various electronic shells it will not be possible to determine to what extent that enhancement of cross sections at large angles is due to inner-shell effects. Some evidence regarding the relative importance of inner-shell electrons and distortion effects may be derived from a comparison of the shapes of the angular distributions for electrons ejected by protons while maintaining the same ratio of electron-to-proton velocity. If the velocity ratios remain constant, one would expect the relative importance of direct proton-electron interactions to be similar at each proton energy. However, the lower-energy protons should cause a greater degree of distortion of the electron distributions, owing to an interaction of longer duration, and, in contrast, the contribution from electrons ejected from inner shells should decrease for lower-energy protons. The shapes of angular distributions for the three proton energies are compared in Fig. 7 for several different ratios v_e/v_p. In order to properly interpret these comparisons several factors must be considered. First, the cross sections are plotted after normalizing the cross sections such that the maximum of each curve for a given velocity ratio has nearly the same magnitude. All cross sections are therefore relative values. Second, the effects of Auger electrons are important for several

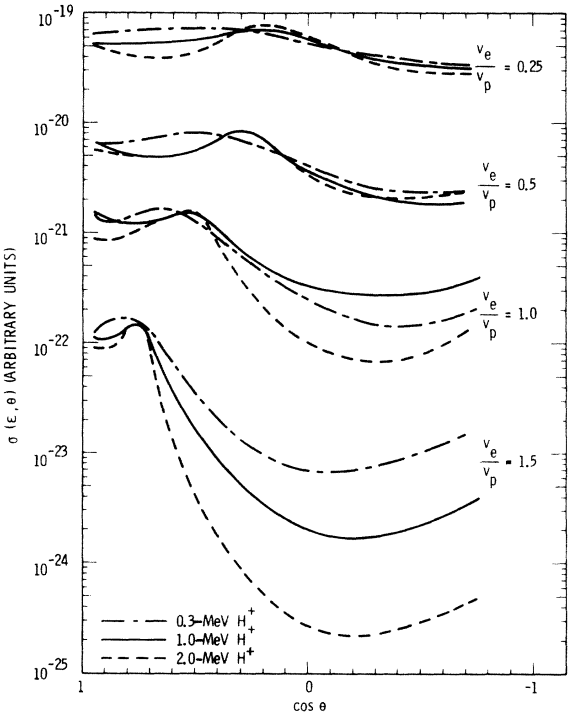

FIG. 7. Angular distributions of electrons ejected from xenon for different proton and electron energies. Curves with similar velocity ratios, v_e/v_p, are normalized together at angles near the binary-encounter peak.

curves. For example, the 1-MeV curve for $v_e/v_p = 1$ corresponds to electron energies of 540 eV, which is in the energy region of the maximum contribution due to the M-Auger spectrum. The Auger electrons will tend to smooth this 1-MeV angular distribution by enhancing large- and small-angle cross sections. Similar effects occur in the 0.3-MeV curve for $v_e/v_p = 0.5$ (40 eV; Coster-Kronig transitions) and the 1-MeV curve at $v_e/v_p = 0.25$ (37 eV; Coster-Kronig transitions). Third, for cross sections at a given velocity ratio the kinematic peak (binary-encounter peak) should occur at the same angle. This prediction is varified by the 1.0- and 2.0-MeV results; however, the 0.3-MeV cross sections peak at smaller angles or, as in the $v_e/v_p = 0.25$ case, hardly any peak is observed. This shift in the peak can be attributed to the effect of atomic binding on the ejected electrons. For the 0.3-MeV protons the ejected-electron energies are quite small for the velocity ratios considered in Fig. 7, and binding energy may cause a relatively large perturbation in the electron-proton interaction.

In Fig. 7 the relative cross sections for electron ejection at large angles are larger for low-energy protons at all velocity ratios, except where Auger transitions dominate the cross sections (these

cases are pointed out above). This result implies that the enhancement mechanism does not rely on inner-shell ionization, which would increase with increasing proton energy. This enhancement of large-angle cross sections appears to be related to distortion of the atomic electron distributions and/or to interference effects. Calculations using Hartree-Fock and/or Hartree-Slater wave functions would be useful to determine the magnitude of interference effects in this energy range.

IV. SINGLE-DIFFERENTIAL CROSS SECTIONS

Cross sections differential in electron energy can be obtained by integration of the measured double-differential cross sections with respect to electron-emission angle. These results can then be compared to calculations performed using binary-encounter theory, which is the only theory presently used for target atoms with multiple shells. The binary-encounter results shown in Fig. 8 were calculated with a program obtained from Rudd.[15] This theory, based on the Gerjuoy-Vriens equations,[16,17] is a semiclassical treatment in which the cross sections are calculated taking into account the relative velocity between the incident proton and the bound electron. The velocity distribution of the bound electrons is assumed to be isotropic with a quantum-mechanical speed distribution deduced from a Fock distribution. Other parameters in the calculation include the ionization potential of each atomic shell or subshell and the ratio γ of the orbital kinetic energy to the ionization potential. In Fig. 8 the results

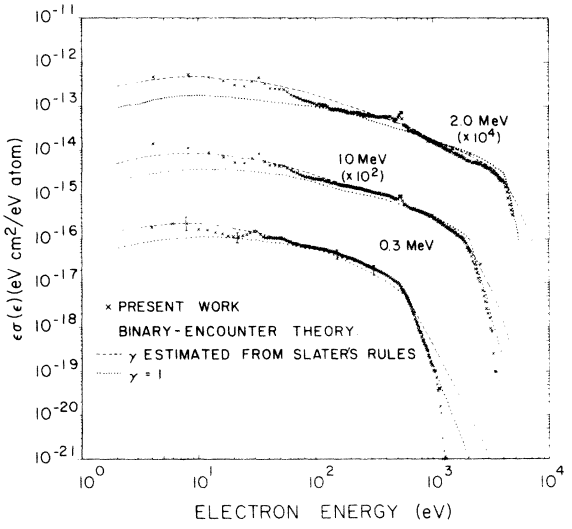

FIG. 8. Cross sections, differential in ejected electron energy, for ejection of electrons from xenon by 0.3-, 1.0-, and 2.0-MeV protons. The binary-encounter theory is from a program supplied by Rudd (Ref. 15).

of two calculations are shown; in one, the orbital kinetic energy was taken equal to the ionization potential, $\gamma = 1$, and in the second, the orbital kinetic energy was estimated by Slater's rules.[18] Previous comparisons of binary-encounter theory with measured spectra for low-atomic-number targets have resulted in agreement to within experimental uncertainty throughout most of the energy range of the electron spectra.[4,6,15] The largest discrepancies have been observed at the low- and high-energy ends of the spectra, where the calculated cross sections are highly dependent on the value chosen for the ratio γ. The binary-encounter cross sections shown in Fig. 8 were obtained by calculating the cross sections for each atomic shell or subshell and adding these results to obtain the cross sections for the atom. The agreement between calculated and measured values is quite good throughout most of the energy range of the ejected electrons. The calculation, using Slater's rules to estimate γ, is in better agreement at low energies, and both calculations overestimate the very-high-energy cross sections. This agreement is satisfying when one considers the number of electronic shells which must be summed to obtain the binary-encounter cross sections. This theory does not, of course, predict the structure in the electron spectra due to Auger electrons except by inference, in that the Auger transitions are a consequence of filling inner-shell vacancies which are predicted by the theory.

V. TOTAL IONIZATION CROSS SECTIONS

By integrating the double-differential cross sections, with respect to both the ejected-electron energy and angle, the total cross section for ionization by proton impact is obtained.

Since electrons ejected by Auger cascades and multiple inner-shell vacancies are included in the measured spectra, the integral performed to obtain the total ionization cross section will contain single- and multiple-ionization contributions. Based on the extent of multiple ionization by fast electrons,[19] the total ionization cross section of xenon obtained from our measured electron cross sections may be as much as 30% larger than the cross section for single ionization. Since there is no information regarding the degree of multiple ionization of xenon by protons in this energy range, and since there are large uncertainties in estimating proton cross sections from electron-impact results, we have chosen to report the total cross sections as determined from our data with no corrections for multiple ionization. Discussion of the magnitude of inner-shell ionization will be deferred to Sec. VI.

The total ionization cross sections obtained by integration of the measured double-differential cross sections are shown in Fig. 9, along with cross sections measured for electron impact (plotted for equal velocities of the incident electrons and protons) and those obtained using binary-encounter theory. Cross sections calculated from binary-encounter theory using $\gamma = 1$ are nearly a factor of 2 smaller than those shown in Fig. 9 which were obtained using γ as estimated by Slater's rules. This difference would be expected since the calculations using $\gamma = 1$ were seen to underestimate the low-energy single-differential cross sections (see Fig. 8), and the low-energy cross sections contribute the major portion of the integral which was performed to obtain the total ionization cross section. The agreement between our measured cross sections and the values calculated using γ obtained from Slater's rules is excellent; however, the dependence on the ratio γ and the fact that binary-encounter theory does not precisely give the shape of the single-differential electron-emission spectra may indicate that the agreement obtained in the total ionization cross section is coincidental.

The comparison of our measured total ionization cross sections with previous measurements of Schram *et al.*[20] for incident electrons shows close agreement where the measurements overlap at 2 MeV (equivalent electron energy of approximately 1 keV). For the lower proton energies, our cross sections are larger than the electron-impact measurements reported by Rapp and Englander-Golden.[21] Previous measurement for low-Z targets have also shown proton cross sections to be larger than electron-impact results for low-energy protons.[22] The differences may be due to variations in the degree of multiple ionization resulting for the different incident projectiles. For low-Z targets the degree of multiple ionization has been shown to increase with decreasing proton energies.[23]

VI. INNER-SHELL IONIZATION AND AUGER ELECTRON EMISSION

Inner-shell ionization can be investigated through Auger electron emission following inner-shell vacancy production. In the present work, M- and N-shell Auger electrons are observed superimposed on a relatively large background produced by direct proton-electron interactions. For incident protons in the energy range of the present measurement, insufficient K- and L-shell ionization was produced to be observed.

When vacancies are produced in the M- or N-shell of xenon, these vacancies are filled either by Auger or Coster-Kronig transitions. The fluorescence yields for the M- and N-shells of xenon may be considered negligible compared to the Auger yield.[24,25] Initial vacancies in the $M_{1,2,3}$ and $N_{1,2,3}$ subshells are efficiently transferred to the $M_{4,5}$ and $N_{4,5}$ subshells, respectively, by Coster-Kronig transitions.[8] Therefore, Auger spectra originating from vacancies in any subshell within the M and N shells will be characteristic of vacancies in the outer subshells. The Auger and Coster-Kronig processes will not be discussed in detail here since they have recently been reviewed extensively by Sevier.[8]

The Auger spectra resulting from M-shell ionization by 2.0-MeV protons are shown in Fig. 9. The energies of the Auger lines and groups of lines designated in Fig. 9 were calculated from the relationship

$$E(M_i N_j N_q) = E(M_i) - E(N_j) - E^*(N_q) \ , \qquad (2)$$

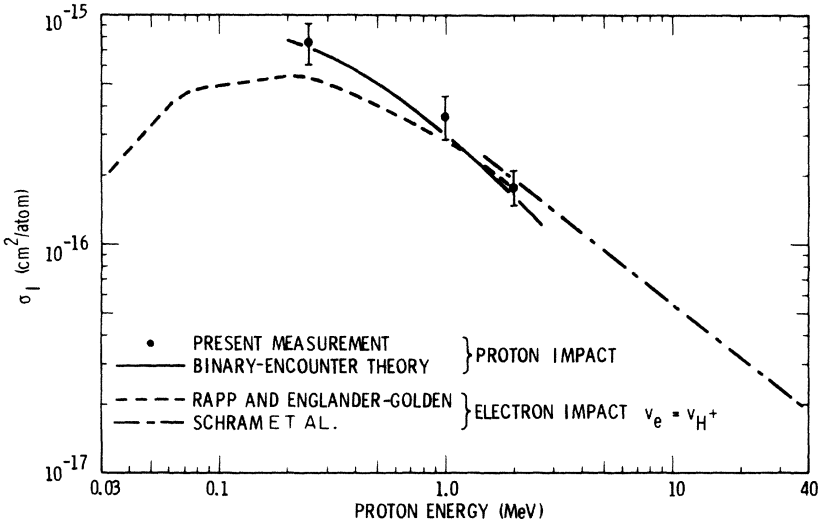

FIG. 9. Total ionization cross sections for ionization of xenon by protons and electrons. The electron-impact cross sections, plotted at velocities equal to the proton velocities, are from Schram *et al.* (Ref. 20) and Rapp and Englander-Golden (Ref. 21). The theoretical calculations are discussed in the text.

where $E(M_i)$ is the binding energy of the M_i electron in xenon, $E(N_j)$ is the N_j electron binding energy, and $E^*(N_q)$ is the binding energy of the N_q electron in an atom with atomic number one larger, in this case cesium. The use of the binding energy of N_q from an atom with atomic number $Z+1$ is an approximate correction for the effect of the inner-shell vacancy on the binding energy of an outer electron due to a change in electron screening of the nucleus.[24] The energies of the M-shell Coster-Kronig transitions were calculated from an expression similar to Eq. (2), except that $E(N_J)$ was replaced by $E(M_j)$. As one can see from Fig. 10, there is a wealth of Auger transitions energetically possible following a vacancy in the M shell of xenon. By drawing on previous work for K-, L-, and M-shell Auger spectra[8] one would expect the MNN Auger transitions to be more probable than the MNO transitions, which in turn would be more probable than the MOO transitions. There does not appear to be evidence of MOO lines in Fig. 9, indicating that the intensity of these lines is sufficiently small that they are lost in the background of electrons resulting from direct proton-electron collisions. We find no evidence of M_1-, M_2-, or M_3-Auger lines; this absence supports our statement that vacancies in inner subshells are transferred to outer subshells by Coster-Kronig transitions before normal Auger transitions occur. The most intense normal Auger lines, which one would expect associated with initial vacancies in the M_1, M_2, and M_3 subshells, if these vacancies were not filled by Coster-Kronig transitons, would occur at approximately 815, 877, and 1022 eV for these shells, respectively. The most intense lines observed within the M-Auger group are attributed to the combined $M_{4,5}N_{4,5}N_{4,5}$ transitions. The energy resolution of the present work (3.5% full width at half-maximum) is not adequate to resolve these lines individually. It should be noted that the measured peaks are slightly lower in energy than may be expected from the transition energies calculated. This difference may result from the effects of additonal ionization of the atom by Coster-Kronig transitions prior to the normal Auger transitions or from the approximate nature of the transition energies calculated with Eq. (2). Due to the large number of possible Auger transitions and the limited energy resolution available, no attempt will be made to identify specific transitions. It suffices to say that the most prominent M-Auger line groups, in order of intensity, appear to be $M_{4,5}N_{4,5}N_{4,5}$, $M_{4,5}N_{2,3}N_{4,5}$, $M_{4,5}N_{2,3}O$, and $M_{4,5}N_{4,5}O$. Of these line groups only the $M_{4,5}N_{4,5}O$ group appears nearly resolved from other groups. The $M_{4,5}N_{2,3}O$ group is identified with the low-energy shoulder on the most intense peak within the spectrum; the principal contribution to the most intense peak is attributed to $M_{4,5}N_{4,5}N_{4,5}$ transitions. An estimate of the ratio of group intensity to total M-Auger intensity was made for three of the line groups with the following results:

$$M_{4,5}N_{4,5}N_{4,5}/\text{tot} = 0.375,$$

$$M_{4,5}N_{2,3}O/\text{tot} = 0.128,$$

$$M_{4,5}N_{4,5}O/\text{tot} = 0.05.$$

Other lines or line groups could not be graphically

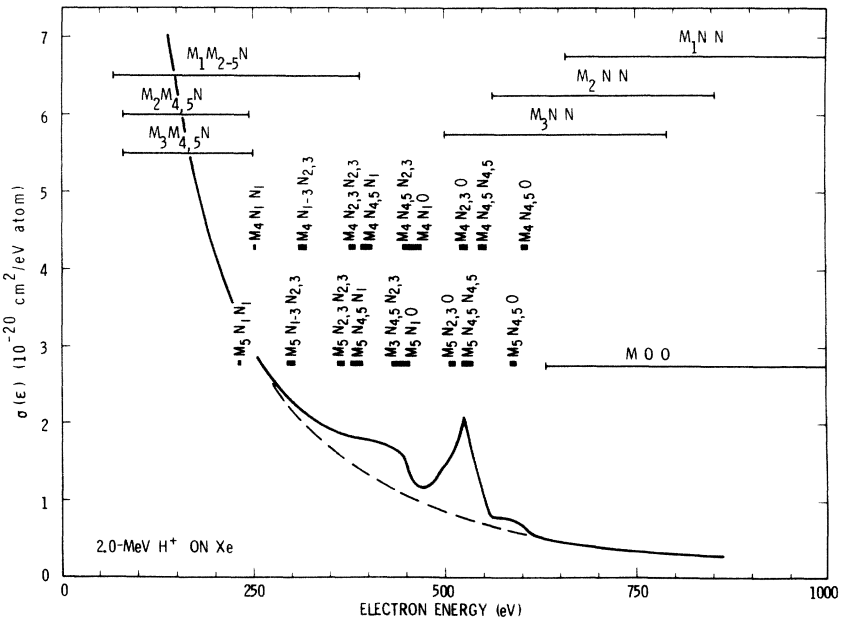

FIG. 10. M-Auger spectrum of xenon. Primary M-shell vacancies were produced by 2.0-MeV proton impact.

resolved unambiguously. It is interesting that the $M_{4,5}N_{2,3}O$ intensity appears larger than the $M_{4,5}N_{4,5}O$ intensity. The shoulder on the side of the $M_{4,5}N_{4,5}N_{4,5}$ peak which is attributed to the $M_{4,5}N_{2,3}O$ transitions may, however, include contributions from $M_{4,5}N_{4,5}N_{4,5}$ transitions that are shifted to lower energies due to multiple ionization of the target atom prior to the Auger transitions. It is possible, for example, that the entire shoulder on this peak is due to such satellite peaks. It is unfortunate that our energy resolution was not adequate for us to resolve these questions in a better fashion.

The Coster-Kronig transitions associated with initial vacancies in the M shell can occur in the energy range from a few eV to several hundred eV. Within this energy region of the ejected-electron spectrum the cross sections for electron ejection by direct proton-electron interactions are very large compared to the probability of producing an M-shell vacancy; thus the continuum background is much larger than the Coster-Kronig peaks which one would expect to see. With the present counting statistics the M-shell Coster-Kronig transitions were lost in the statistical variations of the continuum background.

The transition energies indicated for the N-Auger and N-Coster-Kronig transitions shown in Fig. 11 were calculated from an equation analogous to Eq. (2), where M- and N-subshell notation was replaced by N- and O-subshell notation, respectively. The binding energies presented by Sevier[8] were used in these calculations. Had the binding energies of Hagström *et al.*[26] been used, the energy spread in the calculated positions of each of the three Auger groups shown in Fig. 11 would be increased by approximately a factor of 2. The major difference between the two sets of binding energies is that the N_4-N_5 level separation given by Sevier[8] is 2 eV, whereas Hagström *et al.*[26] report 10 eV. These uncertainties make it difficult to identify the observed structure; however, the group positions shown in Fig. 11 suggest that the most intense portion of the spectrum is associated with $N_{4,5}O_1O_{2,3}$ transitions. This is somewhat unexpected since the $N_{4,5}O_{2,3}O_{2,3}$ line group is analogous to the $M_{4,5}N_{4,5}N_{4,5}$ group, which was found to form the most intense group of the M-shell spectra. It is possible that the approximate method of Auger energy calculation or uncertainties in the N-shell binding energies could result in a shift in the calculated N-Auger transition energies. A 10-eV lowering of the N-shell binding energy necessary to bring the calculated value of the energy of the $N_{4,5}O_{2,3}O_{2,3}$ line group into agreement with the measured position of the most intense group of the N-Auger spectrum would, however, also shift the position of the $M_{4,5}N_{4,5}N_{4,5}$ transitions to higher energies. This shift would result in larger disagreements for the M-shell spectrum between calculated transitions and measured peak positions. It is doubtful that the spectrum is shifted experimentally, since the electron spectrometer has been calibrated to ±2 eV and is probably accurate to ±1 eV in this region of the energy spectrum. Based upon the approximate method of energy calculation used, the major peak in the N-Auger spectrum appears, therefore, to be

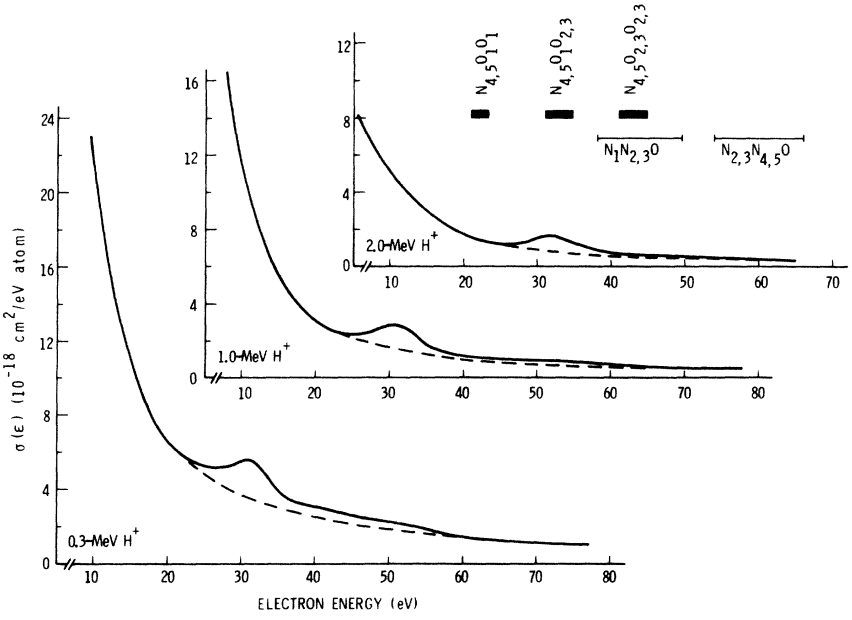

FIG. 11. N-Auger spectrum of xenon. Spectra are shown resulting from ionization by protons of several energies.

associated with the transitions $N_{4,5}O_1O_{1,2}$.

The high-energy tail of the observed N-Auger spectrum, that part of the spectrum between approximately 55 and 60 eV, is attributed primarily to N-shell Coster-Kronig transitions. The ratio of the area of the spectrum from approximately 35 to 60 eV to the total spectral area is approximately 0.3. It is impossible to determine from our data what part of this area is associated with the $N_{4,5}O_{1,2}O_{1,2}$ transitions and what part with Coster-Kronig transitions. One might estimate that at least 50% of the area in this high-energy part of the spectrum is a result of Coster-Kronig transitions, since no Auger transitions are expected with energies greater than about 45 eV.

Although very little quantitative information can be reported concerning line positions and intensities in either the M- or N-shell spectra, these spectra do provide information regarding the probability of inner-shell ionization. It was stated earlier that the fluorescence yield for the M and N shells of xenon is negligible compared to the Auger yield. This observation implies that for each inner-shell vacancy produced by interactions with the incident proton an Auger electron is ejected. One need only count the Auger electrons and infer the total inner-shell ionization cross sections. This procedure has been used successfully for K-shell ionization[27,28] but has additional complications when the inner shells have various subshells. Auger electrons from the M-shell of xenon are energetically possible throughout an energy range of 230–1125 eV. The major portion of these electrons appear in the 230–600 eV region; however, the number which does occur between 600 and 1125 eV is spread thinly over a large region and becomes lost in the statistical background due to other processes. One cannot reduce this background by simply looking at back angles, as in the case of K-shell ionization, because the angular distribution of Auger electrons is not necessarily isotropic for other than K-Auger processes.[8,29] We must therefore measure the cross sections for electron emission at various angles and integrate with respect to angle to determine the energy distribution of Auger electrons. This fact implies that we cannot remove the continuum electron background experimentally. In the case of the M-Auger spectrum, the electron energy is sufficiently high that the continuum background can be approximated quite well by binary-encounter theory. Binary-encounter theory provides cross sections which fit the measured continuum spectra very well, both above and below the energy of the M-Auger spectra, and leads to the dashed line shown in Fig. 10. The total M-shell ionization cross sections were then obtained by integration with respect to electron energy of the Auger spectra between approximately 250 and 700 eV (see Fig. 10) after subtraction of the background indicated by the dashed line. Since a limited energy interval was integrated, and it is possible to have Auger transitions which result in ejection of electrons outside this interval, one must consider these cross sections only as lower limits. The total inner-shell cross sections are shown in Fig. 12, along with results calculated using binary-encounter theory. The theoretical results were obtained from the program discussed earlier, except that in this case only contributions relevant to a particular principal quantum number were summed. The agreement is excellent between calculated and measured M-shell ionization cross sections. However, this agreement may be fortuitous, since the measured values must be considered lower limits and the accuracy of such a simple calculation is questionable.

The N-shell ionization cross sections shown in Fig. 12 were obtained by integration of spectra, as shown in Fig. 11. The background was much more difficult to estimate in the N-Auger case than in the M-shell case previously discussed. The energy range of the N-Auger electrons is

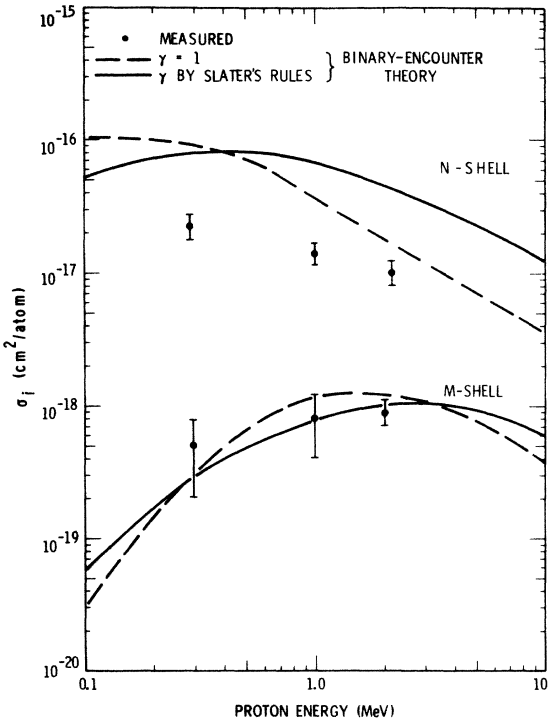

FIG. 12. Ionization of the M and N shell of xenon by 0.3–2.0-MeV protons. The calculated values are from the binary-encounter-theory program of Rudd (Ref. 15).

too low for binary-encounter theory to be reliable as an estimate for the continuum background. The dashed line shown in Fig. 11 is an estimate based on continuum electron distributions measured for several gases which have no Auger electrons in this region and on comparisons with spectra calculated using binary-encounter theory. The entire Auger–plus–Coster-Kronig spectrum was integrated to obtain the N-shell ionization cross section. These cross sections should be corrected to account for the 15–25% contribution due to Coster-Kronig transitions. However, this correction is small compared to other uncertainties, such as an assessment of the continuum background. This uncertainty in the shape of the continuum electron distribution underlying the Auger transitions in this energy range leads to the assignment of large uncertainties in the total N-shell ionization cross sections. The measured values, however, still fall well below the calculated cross sections shown in Fig. 12.

VII. SUMMARY

Double-differential cross sections are presented for electrons ejected from xenon by protons with energies from 0.3 to 2.0 MeV. The principal features of the energy spectra include the kinematic peak which occurs at forward angles as a result of collision of the proton with the atomic electrons, M- and N-shell Auger spectra superimposed on this continuum of electrons from the direct processes, and a maximum in the continuum spectra for very-low-energy electrons ejected in soft (distant) proton-atom collisions.

The angular distributions of electrons of a given ejection energy are much more nearly isotropic for xenon than corresponding electrons ejected from simpler targets such as hydrogen and helium. This result is attributed primarily to interference effects and/or to distortion of the charge distribution of the target atom by the impulsive interaction of the passing proton.

After the cross sections were integrated with respect to emission angle, the energy distributions were compared with binary-encounter theory. Although binary-encounter theory has been shown to provide reasonable results for simple targets (i.e., one or two electronic shells) it was interesting to compare results of this theory with measurements on xenon, which has five principal electronic shells and many subshells. After calculating the probability of electron ejection for each shell and subshell for xenon and adding these contributions to give the total probability for ejection of electrons of a given energy, the results were in agreement with the measured cross sections to within 20–30% throughout most of the energy range of the ejected electrons. The largest discrepancies exist at the low- and high-energy ends of the ejected-electron spectra, which was also characteristic of simple targets. As was shown for simpler target systems, binary-encounter calculations which use $\delta = 1$ provide the best results at the high-energy end of the electron spectra, and the use of δ determined by Slater's rules provides the best results for low-energy electrons.

Total ionization cross sections obtained by integration of the double-differential cross sections with respect to both electron energy and ejection angle were compared with previous measurements for equivalent-velocity incident electrons. The present measurements are slightly larger at the lowest velocities of the incident protons, but in excellent agreement with previous measurements at the higher velocities.

Inner-shell vacancies produced in the M and N shell of xenon are transferred among subshells by Coster-Kronig transitions and result in Auger transitions primarily from the outer subshells. The most prominent peak in the M-Auger spectrum was attributed to $M_{4,5}N_{4,5}N_{4,5}$ transitions with lesser contributions from the $M_{4,5}N_{2,3}N_{4,5}$, $N_{4,5}N_{2,3}N_{2,3}$, $M_{4,5}N_{2,3}O$, and $M_{4,5}N_{4,5}O$. No Coster-Kronig transitions were observed from the M shell. The N-shell Auger spectrum was somewhat simpler, with the major peak attributed to the $N_{4,5}O_1O_{1,2}$ transitions and the remaining high-energy tail associated with $N_{4,5}O_{2,3}O_{2,3}$ Auger transitions and the Coster-Kronig transitions $N_1N_{2,3}O$ and $N_{2,3}N_{4,5}O$.

Inner-shell ionization cross sections were obtained from the M- and N-Auger spectra. The M-shell ionization cross sections are in close agreement with calculations based on binary-encounter theory, whereas the N-shell cross sections are a factor of 2–5 smaller than calculated values.

ACKNOWLEDGMENTS

The author would like to thank J. E. Choate and C. A. Ratcliffe for their help in the operation and maintenance of the Van de Graaff facility. Appreciation is also expressed to W. A. Glass, W. E. Wilson, L. E. Porter, and W. C. Roesch for helpful discussions in the preparation of this paper.

*Paper based on work performed under United States Atomic Energy Commission Contract No. AT(45-1)-1830.

[1]M. E. Rudd and J. H. Macek, Case Studies At. Phys. 3, 47 (1972).

[2]D. H. Madison, Phys. Rev. A 8, 2449 (1973).

[3]S. T. Manson and L. H. Toburen, in *Abstracts of the Eighth International Conference on the Physics of Electronic and Atomic Collisions*, edited by B. C. Čobić and M. V. Kurepa (Institute of Physics, Belgrade, Yugoslavia, 1973), pp. 695 and 696.

[4]L. H. Toburen, Phys. Rev. A 3, 216 (1971).

[5]L. H. Toburen, Phys. Rev. A 5, 2482 (1972).

[6]L. H. Toburen and W. E. Wilson, Phys. Rev. A 5, 247 (1972).

[7]J. B. Crooks and M. E. Rudd, Phys. Rev. A 3, 1628 (1972).

[8]Kenneth D. Sevier, *Low Energy Electron Spectroscopy* (Wiley, New York, 1972).

[9]L. Vriens, Physica 45, 400 (1969).

[10]T. F. M. Bonson and L. Vriens, Physica 47, 307 (1970).

[11]Yong-Ki Kim, Phys. Rev. A 6, 666 (1972).

[12]J. B. Crooks and M. E. Rudd, Phys. Rev. Lett. 25, 1599.

[13]J. Macek, Phys. Rev. A 1, 235 (1970).

[14]A. Salin, J. Phys. B 2, 631 (1969).

[15]M. E. Rudd and D. Gregoire, in *Physics of the One- and Two-Electron Atoms*, edited by F. Bopp and H. Kleinpoppen (North-Holland, Amsterdam, 1969), pp. 795–800; M. E. Rudd (private communication).

[16]E. Gerjuoy, Phys. Rev. 148, 54 (1966).

[17]L. Vriens, Proc. Phys. Soc. Lond. 90, 935 (1967).

[18]B. B. Robinson, Phys. Rev. 140, A764 (1965).

[19]Th. M. El-Sherbini, M. J. Van der Wiel, and F. J. de Heer, Physica 48, 157 (1970).

[20]B. L. Schram, F. J. de Heer, M. J. Van der Wiel, and J. Kistemaker, Physica 31, 94 (1965).

[21]D. Rapp and P. Englander-Golden, J. Chem. Phys. 43, 1464 (1965).

[22]F. J. de Heer, J. Schutten, and H. Moustafa, Physica 32, 1766 (1966).

[23]N. Stolterfoht, Phys. Lett. 41, 400 (1972).

[24]E. J. McGuire, Phys. Rev. A 5, 1043 (1972).

[25]R. W. Fink, R. C. Jopson, Hans Mark, and C. D. Swift, Rev. Mod. Phys. 38, 513 (1966).

[26]S. Hagström, C. Nordling, and K. Siegbahn, in *Alpha-, Beta- and Gamma-Ray Spectroscopy*, edited by K. Siegbahn (North-Holland, Amsterdam, 1965), pp. 846–855.

[27]L. H. Toburen, Phys. Rev. A 5, 2482 (1972).

[28]L. H. Toburen, in *Proceedings of the International Conference on Inner Shell Ionization Phenomena*, edited by R. W. Fink, S. T. Mavson, J. M. Palms, and P. Venugopala Rao (U.S. AEC, Oak Ridge, Tenn., 1972).

[29]B. Cliff and W. Mehlhorn, Phys. Lett. 37A, 3 (1971).